UNIVERSITY OF CALIFORNIA, SAN DIEGO

# Checkpoint gene interactions that suppress genome instability in *Saccharomyces cerevisiae*

A thesis submitted in partial satisfaction of the requirements
for the degree Master of Science

in

Biology

by

Sarah Pang Clotfelter

Committee in charge:

Professor Richard D. Kolodner, Chair
Professor Lorraine Pillus, Co-Chair
Professor Randolph Hampton

2014

The Thesis of Sarah Pang Clotfelter is approved and it is acceptable in quality and form for publication on microfilm and electronically:

---

---

Co-Chair

---

Chair

University of California, San Diego

2014

TABLE OF CONTENTS

LIST OF ABBREVIATIONS

| | |
|---|---|
| **5-FOA** | 5-fluoroorotic acid |
| **dGCR** | Duplication-mediated GCR assay |
| **DKM** | Diploid Killing Media |
| **GCR** | gross chromosomal rearrangements |
| **NAT** | Nourseothricin N-acetyl transferase |
| **SGA** | synthetic genetic array |
| **YPD** | Yeast extract-dextrose-peptone media |

LIST OF FIGURES

LIST OF TABLES

ACKNOWLEDGMENTS

Acknowledgments to Dr. Richard D. Kolodner for serving as chair of this committee and to Dr. Lorraine Pillus and Dr. Randolph Hampton for serving on this committee.

A special thank you to Dr. Kolodner for mentoring me and for allowing me to explore and study cancer biology, and to Anjana Srivatsan for her patient oversight for the past four years. Thank you to Chris Putnam, Sara Bell, Sandra Martinez, Rahul Nene, and Lorraine Yeung for their help with the crossing, patching, and scoring as it was a collaborative effort. Thank you to the rest of the members of the Kolodner Lab: among them Katie Pallis, Catherine Smith, Eric Jaenig, Binzhong Li, Nikki Bowen, Bill Graham, Elaine Guo, Eva Goellner, and Betsy Van Ness.

This work in part includes material currently being prepared for publication: Putnam, Chris; Martinez, Sandra; Srivatsan, Anjana; and Nene, Rahul.

ABSTRACT OF THE THESIS

Checkpoint gene interactions that suppress genome instability in *Saccharomyces cerevisiae*

by

Sarah Pang Clotfelter

Master of Science in Biology

University of California, San Diego, 2014

Professor Richard D. Kolodner, Chair
Professor Lorraine Pillus, Co-Chair

Genome instability, which includes mutations in gene sequences, aneuploidy, and gross chromosomal rearrangements (GCRs), is a common characteristic of cancer. Genome instability can be caused by several genetic defects including defects in DNA damage and replication checkpoint pathways; such defects are also known to play a role in the formation and progression of cancer. However, the cellular pathways that interact with the checkpoint responses to maintain genome stability are not well

understood. To identify such pathways in *Saccharomyces cerevisiae*, double mutant strains were generated by systematically crossing query strains containing a GCR assay (the duplication-mediated GCR assay) and mutations in individual checkpoint genes (*rad17, mec1*, *rad9*, *mrc1, mrc1-aq, rad53*, *chk1,* and *dun1*) with an array of 632 strains containing deletions of individual genes implicated in preventing GCRs. The double mutant strains were then analyzed for GCR formation using a semi-quantitative scoring system. A complex-by-complex approach was used to identify robust interactions. Using this analysis, 20 complexes were identified that interacted with the checkpoint pathways to suppress GCR formation. These 20 complexes included genes involved in DNA repair or the DNA damage response, histone modification and transcription, and other functions. Further mechanistic studies of these complexes can be used to elucidate pathways and interactions previously unknown to suppress cancer-related genome instability.

# INTRODUCTION

## Genome Instability and Cancer

Cancer is characterized by the uncontrolled proliferation of cells. One of the hallmarks of many cancers is genome instability (Hanahan and Weinberg, 2011). Genome instability is manifested as on-going changes in the DNA sequence, loss or gain of entire chromosomes (aneuploidy), and large structural changes in chromosomes (Lengauer et al., 1998). Large structural changes in chromosomes, known as gross chromosomal rearrangements (GCRs), include deletions, duplications, translocations, inversions, and a recently identified mechanism of chromosome shattering and reassembly termed chromothripsis (Chen and Kolodner, 1999; Stephens et al., 2011).

These three categories of genomic instability (mutations, aneuploidy, and GCRs) are not mutually exclusive; cancers that have been extensively characterized tend to exhibit multiple categories of genomic alterations, and one type of genomic instability can give rise to others. For example, some colorectal cancers with hallmarks of sequence instability have been also been observed to have chromosomal structure instability (Abdel-Rahman et al., 2001). Mutational inactivation of genes involved in maintaining either the numerical or the structural stability of chromosomes can link sequence stability to karyotype stability. For example, mutational inactivation of *STAG2*, which encodes a protein involved in chromosome cohesion, gives rise to aneuploidy (Solomon et al., 2011). Aneuploidy itself has recently been linked to causing increased levels of chromosome loss and increased mutation rates in the yeast *Saccharomyces cerevisiae* (Sheltzer et al., 2011).

Consistent with the hypothesis that a mutator phenotype promotes cancer initiation and progression (Loeb, 2001), each category of genomic instability has been implicated as causing genetic alterations that drive carcinogenesis. Sequence changes are well-known to inactivate tumor suppressors or activate proto-oncogenes; for example, missense mutations that activate the function of the K-*ras* gene, have been observed in over 80% of pancreatic cancers (Lengauer et al., 1998). Changes in the number and structure of chromosomes have been well documented cytogenetically for decades (Mitelman, 1991; Lobo, 2008), and are increasingly identified by computational analysis of data generated by whole genome sequencing (Campbell et al., 2008). For example, aneuploidy is observed in glioblastomas (loss of chromosome X) and papillary renal carcinomas (gain of chromosome VII) (Lengauer et al., 1998), and may drive cancers due to the effects of haploinsufficiency and triplosensitivity (Davoli et al., 2013). GCRs that drive carcinogenesis are best characterized in hematopoietic cancers such as leukemias and lymphomas. The most famous and best characterized is the Philadelphia chromosome in chronic myelogenous leukemia that fuses chromosomes 9 and 22 to generate the *BCR-ABL* fusion gene (Nowell and Hungerford, 1960; Rudkin et al., 1964). The role of the large numbers of GCRs observed in other cancers are less well understood, and although some of these alterations may drive cancer formation (Fouladi et al., 2000; Reid et al., 2012; Saunders et al., 2000), others may simply be "passengers" that are clonally selected during carcinogenesis (Greenman et al., 2007). But regardless of the selective effect of any particular change in the cancer genome, increased rates of genome instability increase the chances of obtaining cancer-promoting alterations (Loeb, 2001).

**DNA Damage and Replication Checkpoint Genes**

Damage to DNA includes base damage and single- or double-stranded breaks that can impede replication and lead to missegregation of chromosomes during cell division. An important cellular mechanism that prevents DNA damage from causing harmful effects is the checkpoint response. DNA damage checkpoint pathways are triggered by DNA damage, aneuploidy, stalled replication forks, and delay or block the cell cycle transitions from G1 to S phase or G2 to M phase to allow sufficient time for DNA repair to occur. During S phase, a DNA damage checkpoint pathway (the intra-S checkpoint) slows replication and cell cycle progression in response to DNA damage. A second S-phase checkpoint, the replication checkpoint, detects replication stress and inhibits the firing of late replication origins and blocks the cell cycle (Putnam et al., 2009b; Zhou and Elledge, 2000). The *S. cerevisiae* genes involved in the various checkpoint pathways have been identified and are highly conserved across organisms (*Figure 1*). The checkpoint proteins fall into 3 main categories: sensors, adaptors, and effectors (*Figure 1*) (Harrison and Haber, 2006; Kolodner et al., 2002; Putnam et al., 2009b). The sensors detect DNA damage and include the kinases encoded by *MEC1* and *TEL1*, the proteins that form a clamp on damaged DNA, encoded by *RAD17*, *MEC3* and *DDC1*, and repair/replication proteins involved in recruiting the sensor kinases, such as RPA and the Mre11-Rad50-Xrs2 complex. The sensor kinases activate the effector kinases encoded by *CHK1* and *RAD53*; activation of Rad53 involves phosphorylation of the Rad53 kinase as well as phosphorylation of either of the Rad53 adaptor proteins encoded by *RAD9* and *MRC1* (Harrison and Haber, 2006; Putnam et al., 2009b). The effector kinases function by phosphorylating their substrates, leading to cell-cycle arrest, and either activating or

repressing pathways to allow for repair of the DNA and recovery of the cell (Putnam et al., 2009b). The sensor-adaptor-effector signal cascade does not always function in a linear manner. For instance, the requirement for the adaptors *MRC1* and *RAD9* can be bypassed by the direct activation of Rad53p by Mec1p under specific circumstances (Lee et al., 2004). Therefore, the interactions between the checkpoint genes are complicated and further study is required to comprehensively understand these interactions. Furthermore, their impact on genome stability has not been completely elucidated.

In humans, defects in checkpoint genes have been detected in sporadic tumors and conditions with predispositions to cancer. For example, defects in the human genes *ataxia telangiectasia mutated* (*ATM*) and *ATM*-related, *ATR* (in bladder cancer and childhood leukemia), and the tumor suppressor *p53* are all involved in tumorigenesis (Lengauer et al., 1998; Morris et al., 2010; Yuan et al., 2013). Many of the human checkpoint genes are highly conserved in eukaryotes and have homologs in *S. cerevisiae* that have been extensively studied (*Figure 1*)(Kolodner et al., 2002). Studies in *S. cerevisiae* revealed that mutations that disrupt the replication and DNA damage checkpoints significantly increase the rate of GCRs (Kolodner et al., 2002). Whereas the DNA damage checkpoint genes (*RAD24*, *MEC1*, *RAD9*, *RAD53*, *DUN1*) mainly suppress the unique sequence-mediated GCRs, the replication checkpoint genes (*MRC1*, *TOF1*) suppress GCRs mediated by repeated sequences (Putnam et al., 2009b). The mechanisms by which inactivation of these genes leads to the formation of GCRs are still unclear. Identifying the interactions of these genes with other genes in the checkpoint pathways as well as other pathways will provide insight into the mechanisms underlying GCR formation and help elucidate the network of genes that suppress genome instability.

**Assay to Study GCRs in Yeast**

The original GCR assay was developed and published by Chen and Kolodner in 1999 (Chen and Kolodner, 1999). This assay allowed the detection of GCRs by the loss of counter-selectable markers on the terminal non-essential region of chromosome V-*CAN1* and *URA3*, which confer sensitivity to the drugs canavanine (Can) and 5-fluoroorotic acid (5-FOA), respectively. Therefore, the cells in which these markers are inactivated or lost by chromosomal rearrangements can be recovered because they are no longer sensitive to the two drugs. Two markers were used instead of only one because the frequency of GCR formation is higher than the frequency of mutations that inactivate both markers simultaneously. Thus, the cells that are resistant to both Can and 5-FOA have likely undergone GCRs rather than point mutations in the two genes (Chen and Kolodner, 1999). This method has since been expanded as explained in a paper by Putnam et al. in order to select for GCRs specifically mediated by repeated sequences (Putnam et al., 2009a). In that study, the authors placed the *CAN1* and *URA3* markers downstream of a segmental duplication in the non-essential region on chromosome V (Putnam et al., 2009a). The segmental duplication on chromosome V shares sequence homology to regions on chromosomes IV, X and XIV (Putnam et al., 2009a). It was shown that these duplicated sequences on non-homologous chromosomes undergo recombination, leading to chromosomal translocations, i.e. GCRs at a higher rate than the original assay (Putnam et al., 2009a). This assay was referred to as the duplication-mediated GCR assay (Putnam et al., 2009a), which was manipulated for use in this study.

**Project goals**

This project systematically probed interactions between the DNA damage checkpoint response and other pathways to identify interactions that suppress the formation of GCRs in the genetically tractable *S. cerevisiae*. In order to identify these interactions, query strains, which contained mutations in DNA damage checkpoint genes and a genetic assay for GCR formation, were crossed to a subset of the systematic yeast deletion collection, and haploid progeny were isolated using a modified synthetic genetic array (SGA) protocol (Tong and Boone, 2006; Tong et al., 2001; Tong et al., 2004). The selected haploids contained the DNA damage checkpoint gene mutation, the mutation from the systematic deletion collection, and the genetic assay for GCR formation. These double mutation-containing haploids were then tested for levels of genome instability, and candidate interactions were identified when the observed level of GCR formation of the double mutant strain was higher than that of either single mutant. Candidate interactions were prioritized using the density of genetic interactions involving genes in known pathways and known complexes for further study in *S. cerevisiae* and for characterization in human cancer cell lines and genomic data derived from human tumors.

# METHODS

## Construction of strains

Mutations of checkpoint genes were introduced into the systematic query strain RDKY7635 that was constructed for systematic mating. This strain also contains the duplication-mediated GCR assay (MATalpha *hom3-10 ura3Δ0 leu2Δ0 trp1Δ63 his3Δ200 lyp1::TRP1 iYFR016c::$P_{MFA}$-LEU2 can1::$P_{LEU2}$-NAT yel072w::CAN1-URA3 cyh2-Q38K)*. The endogenous CAN1 gene in this strain was deleted using the nourseothricin-resistance marker (*can1::$P_{LE2}$-NAT)*. Because deletions of the *RAD53* and *MEC1* genes are lethal without deleting the *SML1* gene, which encodes the ribonucleotide reductase inhibitor (Zhao et al., 1998), the *SML1* gene was first knocked out using homologous recombination-mediated gene replacement with a hygromycin resistance cassette amplified from the pFA6a-hph-NT1 plasmid (Janke et al., 2004) to generate the strain RDKY8307 (MATalpha *hom3-10 ura3Δ0 leu2Δ0 trp1Δ63 his3Δ200 lyp1::TRP1 iYFR016c::$P_{MFA}$-LEU2 can1::$P_{LEU2}$-NAT yel072w::CAN1-URA3 cyh2-Q38K sml1::hph)*. The *RAD53* and *MEC1* genes were then separately knocked out in RDK8307 using a *HIS3* marker amplified from pRS303 (Sikorski and Hieter, 1989) to generate RDKY8047 and RDKY8045, respectively. Other RDKY7635-derived query strains used in this study, *rad17::HIS3* (RDKY8049), *rad9::HIS3* (RDKY7719), *mrc1::HIS3* (RDKY7636), *mrc1-aq.HIS3* (RDKY8044), *chk1::HIS3* (RDKY7984), and *dun1::HIS3* (RDKY7784), were already available in the Kolodner laboratory.

## Systematic strain construction

In brief, the wild-type (WT) query strain RDKY7635, containing the GCR assay (MATalpha *yel072w::CAN1-URA3)* and its derivative query strains containing individual mutations in checkpoint genes, were crossed to a subset of the *S. cerevisiae* systematic deletion collection (*Figure 2*). This subset of 632 gene deletions were chosen from a previous bioinformatics screen (Putnam et al., 2012). Each was deleted by replacement with a G418-resistance cassette in the BY4741 background (MATa *his3Δ1 leu2Δ0 met15Δ0 ura3Δ0)*.

First, the deletions, which were previously arrayed in liquid cultures in a 96 well format, were spotted onto yeast extract-peptone-dextrose (YPD)-agar plates using a RoToR robot (Singer) and grown for 2-3 days at 30 °C to form colonies. These colonies were then used to inoculate 120 μL of liquid YPD in 96-well plates. The plates containing these liquid cultures were then sealed with a membrane that was porous to air, and grown overnight at 30 °C with vigorous shaking. The MATalpha query strains were grown in individual 15 mL liquid YPD cultures overnight at 30 °C and then spotted onto YPD agar plates using the robot. The MATalpha query strains were mated with the MATa strains containing the target deletions by overlaying the spots from the respective YPD plates onto fresh YPD plates. The plates were incubated at 30 °C for 2 days to allow strains to mate. The resulting mixture of haploid and diploid strains was then spotted using the RoToR robot onto plates of solid Diploid Selection Medium and grown for 2 days at 30 °C to select for diploids. The diploid selection process was repeated twice. The Diploid Selection Medium was YPD-agar containing 200 ug/mL G418 and 100 ug/mL NAT to select for diploids, which should have the G418-resistance cassette from the

systematic deletion collection strain as well as the NAT-resistance cassette in the *can1* deletion from the query strain.

Haploids were obtained by sporulating the resulting diploids and by then selecting haploids of the desired genotypes. First, diploids that were resistant to G418 and NAT were transferred using the robot from Diploid Selection Medium to Pre-sporulation Medium (containing Difco nutrient broth, 5 g/0.5 L yeast extract, and 5% glucose) for two days at 30 °C. From Pre-sporulation Medium, the cells were transferred to Sporulation Medium using the RoToR robot and then grown for seven days at 30 °C. Sporulation Medium is agar containing potassium acetate (10g/L), zinc acetate (0.05 g/L), G418 (50 μg/mL), and NAT (25 μg/mL). Diploids were then killed by transferring the cells from Sporulation Medium to Diploid Killing Medium (DKM). The DKM contains yeast nitrogen base without amino acids and without ammonium sulfate to ensure the cellular uptake of the aminoglycoside antibiotics used. Glutamic acid (1.0 g/L) was used as a nitrogen source instead of ammonium sulfate. In addition, the DKM contained an amino acid drop-out mix lacking lysine, leucine, and uracil, 50 μg/mL thialysine (to kill cells expressing a wild-type *LYP1* gene), 10 μg/mL cycloheximide (to kill cells with a wild-type *CYH2* gene), glucose (2%), 200 μg/mL G418, and 100 μg/mL NAT. This step represents the main difference between this SGA protocol an the original protocol (Tong and Boone, 2006). The diploid-killing step in the original protocol involved using canvanine to kill diploids, but this is not suitable for our screen because of the use of *CAN1* as a selectable marker in the GCR assay. Therefore, our diploid-killing step involves cycloheximide and thialysine in order to kill diploids. The cells were grown overnight on DKM at 30 °C, and this process was repeated once before transferring the

cells to Haploid Selection Medium using the RoToR robot. The Haploid Selection Medium contains yeast nitrogen base without amino acids and without ammonium sulfate, L-glutamic acid, 2% glucose, an amino acid drop out mix lacking leucine and uracil, and contained 200 μg/mL G418, and 100 μg/mL NAT. Finally, the haploid strains were transferred into a YPD agar plate using the robot and incubated at 30 °C for 2 days. The strains were then inoculated in 120 μL of liquid YPD in 96-well plates using the robot, and the plates were grown overnight in a 30 °C platform shaker. The cells were then mixed with an equal volume of 40% glycerol and stored at -80 °C.

**Haploid screening**

The systematically generated haploids containing the GCR assay, the query checkpoint mutation, and the target mutation were streaked out to a YPD-agar plate to isolate individual colonies. Once the mating was complete, the cells were patched by selecting a single colony with a toothpick and spreading the cells onto a YPD plate, creating a patch. At least three colonies were picked for each strain to obtain at least three patches. The plates were incubated at 30 °C for two days, and then the patches were replica plated onto Can 5-FOA media (60 mg/L Canavanine and 1 g/L 5-fluoroorotic acid) to select for cells that have undergone a GCR event and lost the *CAN1* and *URA3* genes (which confer sensitivity to canavanine and 5-FOA, respectively) (*Figure 3)*. A semi-quantitative method was used to analyze GCR formation in each strain by giving each patch a score based on the number of papillae that grew on the Can 5-FOA medium and averaging the scores (*Figure 4)*. Pictures of the 5-FOA Can plates were taken on the third, fourth, and fifth days to monitor the growth of papillae on the plates. Increases or

decreases in GCRs were semi-quantitatively assessed by examining the number of colonies formed on the double drug containing plates, which is proportional to the number of GCR events that occurred.

**Growth analysis**

Cells were grown to log phase in liquid YPD medium in a 30 °C shaker and diluted in 25 mL of fresh YPD medium to an optical density (OD) of 0.05 at 600 nm. The OD was measured approximately every 90 minutes using a Nanodrop spectrophotometer. The doubling time was determined by plotting the $\log_2$(OD) over time.

**Flow cytometry**

Flow cytometry was used to determine the ploidy of the double mutant cells. Cells were grown first on yeast extract-peptone-dextrose (YPD) plates for 2 days at 30 °C and then inoculated in 4 ml liquid YPD medium overnight at 30°C with vigorous shaking. After ~16 hours, 150 µl of culture was inoculated in 3 ml of fresh liquid HYPD medium, and the cells were grown to log phase (3 hours) in a 30 °C shaker. 200 µl of the cell culture were then centrifuged (14000 rpm for 30 seconds), washed with 200 µl water, centrifuged similarly, and resuspended in 300 µl water, and then fixed with ethanol at a final concentration of 70%. These were then incubated at room temperature for 1 hour. The cells were then pelleted and resuspended in 50 mM sodium citrate, pH 7.0, then sonicated (five 1-second pulses) to break up large aggregates and then pelleted. The cells were then resuspended in 1 ml of sodium citrate buffer containing 1 mg/ml Proteinase K

(Sigma) and 250 μg/ml RNase A (U.S. Biochemicals) and incubated overnight at 37 °C. The cells were then pelleted and resuspended in 1 ml sodium citrate buffer with 1 μM Sytox Green (Molecular Probes) and incubated for one hour in the dark at room temperature. The DNA content was measured using a BD Flow Cytometer.

**Determining rates using fluctuation tests**

To determine the rate of simultaneous inactivation of the *CAN1* and *URA3* genes, fluctuation analysis was performed (Lea and Coulson, 1949b). Strains were streaked out on YPD plates and grown for 2 days. Nine isolated colonies were cut out from the plates to ensure the entire colony was obtained, inoculated in 5 ml of liquid YPD medium, and grown at 30°C with vigorous shaking until the cultures were saturated. These were then plated on to YPD plates and plates containing both 5-fluoroorotic acid (5-FOA) and canavanine (Can). For YPD plates, 0.1 ml of $10^{-5}$ dilutions of the 5 ml cultures were plated. For 5FOA Can plates, an appropriate volume was plated to obtain a countable number of colonies on the plate. This volume was estimated based on the GCR score of the strain, and varied between 0.05 ml to 0.3 ml. The colonies on each YPD and GCR plate were counted, and the rate was calculated as previously described (Putnam and Kolodner, 2010).

# RESULTS

## Experimental design – GCR assay

In order to screen for mutations that caused increased genome instability in combination with mutations in the checkpoint genes, double mutants were generated systematically. The three crucial aspects of the experimental design were the genetic assay for identifying GCR formation, the modified systematic strain construction protocol, and the strategy for analyzing the results.

The assay for GCR formation used in this project was derived from the "duplication-mediated" GCR or dGCR assay published in 2009 (Putnam et al., 2009a) that was modified from an earlier GCR assay (Chen and Kolodner, 1999). These GCR assays detect rearrangements that lose the *CAN1* and *URA3* markers placed on the non-essential terminal region of the left arm of chromosome V. Loss of function of both genes confers resistance to the drugs canavanine (Can) and 5-fluoroorotic acid (5-FOA). Two markers were used instead of only one because the frequency of GCR formation is higher than the frequency of mutations that inactivate both markers simultaneously. Thus, the cells that are resistant to both Can and 5-FOA have likely undergone GCRs rather than point mutations in the two genes.

In the dGCR assay, the *CAN1* and *URA3* markers are telomeric to a segmental duplication in the non-essential region on chromosome V, which shares substantial sequence homology (~2-5 kb) to regions on chromosomes IV, X, and XIV (Putnam et al., 2009a) *(Figure 3)*. These duplicated sequences promote GCR formation by non-allelic homologous recombination, resulting in GCRs that are chromosomal translocations between chromosome V and chromosomes IV, X, or XIV (*Figure 3)*. The propensity to

form these kinds of rearrangements increases the basal GCR rate relative to versions of the assay that do not involve segmental duplication. Importantly, the increased rate is sufficiently high to allow GCR formation to be followed using patch tests and thus allows rapid screening of the systematically generated double mutant strains constructed here.

The direct analysis of the double mutant strains for the accumulation of GCRs by patch testing is a crucial aspect of the experiment. In many other experiments involving systematically generated strains, more easily measured features, such as growth defects, are monitored. In our analysis, however, monitoring of other more easily measured features as "surrogates" for GCR formation would not provide a measure of the formation of GCRs.

**Experimental design – systematic mating**

The systematic strain construction protocol was derived from the synthetic genetic array (SGA) protocol (Tong and Boone, 2006; Tong et al., 2001; Tong et al., 2004), which allows double mutant generation via selection and robotic yeast handling. The genotypes of the query strains and the selection scheme were modified in order to accommodate introduction of the GCR assay in the haploid progeny, which is incompatible with the standard SGA protocols that use canavanine to select against diploids containing a wild-type *CAN1* gene and for haploids with a mutant *can1*. Details of the systematic strain construction are detailed in *Figure 2* and in the Materials and Methods section.

Eight query strains, each containing a mutation in a checkpoint gene, were constructed for systematic mating to generate double mutant strains (*Figure 2)*. Query

strains contained a deletion of the central effector protein kinase *RAD53*; deletions of the partially redundant activators of *RAD53*: *RAD9* and *MRC1*; the *mrc1-aq* allele, which specifically affects the checkpoint function of *MRC1* but is replication proficient (Osborn and Elledge, 2003); deletion of the upstream kinase gene *MEC1*; deletion of the DNA damage sensor *RAD17*, and deletions of the downstream effectors *CHK1* and *DUN1*. Most of the genes selected for study here have well-characterized human homologs that play roles in the DNA damage checkpoint in human cells (*Figure 1B*).

Because the identification of double mutant combinations that cause increased genome instability requires substantially more effort than the identification of synthetic growth defects, we did not cross the eight query strains against the entire deletion collection. Rather, 632 mutations in target genes were selected and arrayed for crossing, which corresponded to ~13% of the ~4,700 non-essential genes in the yeast genome. These 632 genes were identified in a previous *in silico* screen (Putnam et al., 2012) and were prioritized based on their similarity to known GCR-suppressing genes (sensitivity to DNA damaging agents and similar genetic interactions). Importantly, ~90% of the strains in this subset of the systematic deletion collection were verified by PCR; about ~5-10% of strains tested in our copy of the deletion collection were incorrect and had to be reconstituted for use in our analysis. I additionally added mutations not present in the deletion collection, such as *mec1 Δ sml1 Δ, and mrc1-aq*. In addition, I introduced a *leu2::G418* strain in the deletion collection to replace the *leu2 Δ0* already present in the BY4741 background. Haploids containing the *leu2::G418* marker could be isolated, unlike crosses to the wild-type BY4741, which lacks resistance to G418. These *leu2::G418* haploids (labeled as control or *leu2Δ* hereafter) were used as control strains

that were equivalent to a result of a cross to the wild-type BY4741. Crossing the eight checkpoint query strains against the 632 target strains and selecting for double-mutant haploids with the GCR strain resulted in 4,649 haploid double mutant strains (~92% of the attempted double mutants were obtained).

**Experimental design – data analysis**

The strains obtained from the systematic mating were analyzed by patching (as described under Materials and Methods), and each patch was assigned a GCR score. The scores were assigned relative to the wild-type score (~1). Strains with increased numbers of papillae were assigned scores of 2-5, and those with no papillae were given a score of 0 (*Figure 4)*. A score for each strain was then assigned based on the average of the scores from each observed patch, which for the *leu2Δ* control strains could be over 100 patches as three control patches were placed on every plate. The control strain had an average score of 0.97. Although this score is semi-quantitative, a good correlation was observed between the score and the quantitative GCR rate measured by fluctuation analysis. Several mutations caused increased GCR scores in combination with the checkpoint mutations. All the data were tabulated in a spreadsheet and analyzed as follows.

A global spreadsheet was generated that contained the average single and double mutant scores for all strains obtained using systematic mating. To facilitate analysis of the scores, individual cells on the spreadsheet were colored in shades of red based on the magnitude of increase of the double mutant score relative to the higher of the two single mutant scores (*Figure 5*). Decreases were similarly highlighted in shades of blue (*Figure 5*).

Previous analysis of the single mutant scoring data as well as over 90 quantitative rates measured by the fluctuation assay in the Kolodner laboratory allowed identification of an optimal cutoff score that minimized the number of false positive and false negative candidates among the single mutants. This cutoff score was identified to be a score of 0.4 above the score of the *leu2Δ* single mutant control strain, which was 0.98.

For double mutant analysis, the relative effect of each associated single mutant is important. For example, the *dun1Δ hos2Δ* double mutant strain has an averaged GCR score of 2.0, which is substantially above the GCR score of the wild-type strain, 0.98. This score, however, does not indicate a genetic interaction between the *DUN1* and *HOS2* genes as the average GCR score of the *dun1Δ leu2Δ* strain is 2.12 and the average GCR score of the *hos2Δ* strain is 1.0. In general, most double mutant combinations studied here did not substantially alter the GCR score relative to the higher of the two associated single mutant strains. Thus, to identify an interaction, we demanded that the double mutant score be at least 0.4 higher than the higher of the two GCR scores of the associated single mutant strains.

In addition to these criteria, I also sought to use the known biology of the bait genes to distinguish between potential noise and robustly indicated interaction. To do so, sought out sets of clear GCR candidate interactions between the checkpoint genes and genes encoding the subunits of a complex and or components of a pathway (*Figure 5*). Some groups of genes (involved in a complex or pathway) did not show a robust interaction with the eight checkpoint genes tested here and were ignored. Other groups had candidate interactions with multiple checkpoint genes, such as casein kinase II. Other complexes such, as the SWR1 complex, demonstrated an especially high number of

interactions with *mrc1* as well as *mec1*, but less so with the other checkpoint mutations. This screen provides a large variety of potential interactions between checkpoint genes and candidate complexes for further study that may provide novel information about genes that maintain genome stability through interaction with checkpoints. In total, twenty candidate complexes and pathways, which indicated interaction with checkpoints based on the double mutant scores and multiple criteria were identified and included complexes involved in DNA repair and DNA damage response, as well as histone modification and transcription (*Table 4, Table 5)*.

**Validation of the results**

Strains in several groups or complexes that showed high interactions with more than checkpoint were repatched to check the GCR scores. Fluctuation tests were used to determine the rate of GCR formation (Lea and Coulson, 1949a; Putnam and Kolodner, 2010). This method, though more time consuming, allows for a more quantitative analysis of the rate of GCRs. Strains with particularly high interactions with many of the checkpoint genes were picked to perform fluctuation tests to determine if the increase in GCRs were real or false positives. This test enabled the validation of several complexes that were implicated based on patch scores (*Table 2*). Some of the candidate strains with high interaction scores were also analyzed for their ploidy using flow cytometry (*Table 3)*. Some strains, particularly many of the double mutant *rad53* strains were found to be diploids rather than haploids, and therefore could be excluded from the results. The doubling times of the single mutant checkpoint strains showed *rad53sml1* to have a

significantly longer doubling time than the wild-type, consistent with what was observed during the screening process.

# DISCUSSION

In this project, I performed a screen to identify genes and pathways that interact with the DNA damage and replication checkpoint genes to suppress genome instability in *S. cerevisiae*. I crossed 632 candidate target mutants with 8 query checkpoint mutants and obtained 4,649 haploid double mutant strains. Each strain was patched (15,136 patches), and each patch was assigned a score based on the number of drug-resistant papillae that were observed. The averaged scores for each strain were then analyzed with an emphasis on identifying complexes and pathways that showed significant interactions with the checkpoint mutations. Analysis of the GCR scores identified twenty complexes (including casein kinase II, RNase H2, and the Swr1 complex) that interacted with the checkpoint genes. Selected interactions were validated by re-patching the corresponding single- and double-mutant strains and analyzing their ploidy. The GCR rates were quantitatively measured in 10 selected double mutant strains to validate the increased GCR scores. These data reveal that multiple cellular pathways cooperate with the checkpoint response to prevent GCR accumulation.

A previous genome-wide screen (Smith et al., 2004) to identify suppressors of GCR formation used a GCR assay that had a very low basal rate ($3.5 \times 10^{-10}$) (Chen and Kolodner, 1999); therefore, the previous screen required the introduction of a sensitizing mutation, *pif1-m2*, that elevated the baseline rate, but strongly biased the type of GCRs formed to be *de novo* telomere additions. This study also focused entirely on single mutants that increased the GCR rates (in combination with the *pif1-m2* allele) and by its design could not identify genetic interactions required for suppressing GCRs. The duplication-mediated GCR assay has a sufficiently high baseline rate ($8.58 \times 10^{-8}$), which

makes it amenable for use in a systematic screen. Furthermore, the screen was performed against an enriched target mutant set (Putnam et al., 2012), which enabled the rapid identification of a large number of genetic interactions. Another important feature of this screen is that I directly monitored GCR formation, instead of using indirect indicators of genetic interactions such as growth defects. Furthermore, multiple controls were implemented during data analysis, as described below.

The main limitation of this screen is that the growth rate of the strains impacts the number of papillae formed on selective plates, thus influencing the GCR patch score. Therefore, when two mutations in combination cause a growth defect (synthetic growth defect), the double mutant strain would have an artificially low GCR score. An example of this effect was in the case of strains containing the *rad53* deletion. The *rad53* single mutant strain had a significant growth defect (doubling time 136 mins vs. control 99 mins; *Table 1*), and the scores of the rad53 double mutant strains were consistently lower. Another caveat is that despite the diploid killing and haploid selection steps during systematic double mutant generation, some diploid strains are able to survive. These diploids have invariably proven by PCR and sequencing (unpublished data, C.D.P. and R.D.K.) to have undergone gene conversion events (or are reduction in copy number) for regions under selection and are most readily identified by determining ploidy by measuring DNA content by flow cytometry. These strains are expected to have low scores because both copies of the *CAN1-URA3* cassette would have to be lost for them to form papillae on Can+5-FOA plates. Thus, the ploidy of the strains was measured during validation to verify that the strains were haploid (*Table 3*). Another quality control step included testing if GCR scores were consistent when the same double mutant was

obtained in independent reciprocal crosses, e.g. where the mutation used as a query in the first cross is the mutation used as a bait in the second cross.

GCR formation involves multiple steps including the generation of DNA damage (caused endogenously during the course of cellular metabolism, or exogenously, via DNA damaging agents), sensing of the damaged DNA, DNA repair processes that act on the damage, and processing of the damage in a manner that produces GCRs. The complexes and pathways identified in this screen can function at one or more of these steps and cooperate with the checkpoint response to maintain genome integrity. Therefore, in the absence of a normal checkpoint response, exacerbating DNA damage and/or a defect in the cellular response to endogenous metabolic DNA damage would result in elevated genome instability. Further studies are required to elucidate how each of the identified complexes cooperates with the DNA damage checkpoint to maintain genome integrity.

This screen identified twenty groups of genes that showed robust interactions with the checkpoint genes. Interestingly, these groups were enriched in DNA repair pathways including DSB processing (*exo1*, *sae2*), recombination (*rad51*, *rad59*), and non-homologous end joining (*yku70* and *yku80*). Other interesting groups included several complexes involved in chromatin modification and remodeling (Swr1 complex, Isw1a complex), transcription (RNA polymerase I and II transcription), and the RNase H2 complex. These criteria used to select complexes for further analysis rather than individual genes reduce the risk of false positive results. A few novel and unexpected findings are discussed below.

An unanticipated finding was the interaction between *CKB1* and *CKB2* and checkpoints. These genes encode the regulatory subunits Ckb1 and Ckb2, respectively, of the highly conserved casein kinase II (CK II) enzyme, a Ser/Thr protein kinase (Bidwai et al., 1994). This enzyme promotes the transcription of several genes (Ackermann et al., 2001), and is involved in repressing RNA Pol III-mediated transcription in response to DNA damage (Ghavidel and Schultz, 2001). The catalytic subunits of CK II are essential for survival in *S. cerevisiae* (Padmanabha et al., 1990). Interestingly, CK II levels are found to be elevated in tumors (Landesman-Bollag et al., 2001; Munstermann et al., 1990), consistent with the hypothesis that this enzyme promotes cell survival and proliferation. There is evidence that Ckb2 is involved in adaptation, a process wherein cells arrested due to persistent DSBs are able to overcome cell cycle arrest and divide to form microcolonies (Guillemain et al., 2007; Toczyski et al., 1997). In this screen, the *ckb1* and *ckb2* mutations caused increased GCR scores in combination with many checkpoint mutations (*Figure 5*). It is not readily apparent how a defect in adaptation would cause a further increase in GCR formation in the absence of a functional checkpoint response. This suggests that the role of CK II is more complicated than previously believed and perhaps involves additional functions beyond adaptation. Further studies will be required to elucidate the mechanism by which Ckb1 and Ckb2 promote genome stability in the absence of a normal checkpoint response. For instance, it will be interesting to study if CK II kinase activity is required to maintain genome integrity or whether the regulatory subunits have other unidentified roles independent of CK II activity or interact with other proteins.

Another interesting observation was the strong interaction between subunits of the Isw1a complex (IOC3 and ISW1) with multiple members of the DNA damage checkpoint pathway (*Figure 5*). The Isw1a complex is involved in nucleosome spacing (Tsukiyama et al., 1999) and repression of transcription initiation (Vary et al., 2003). Isw1 is an ATPase subunit of a class of chromatin remodelers called imitation-switch. Isw1 was observed to undergo DNA damage-induced phosphorylation by Mec1 and Tel1 (Chen et al., 2010). Isw1 forms the Isw1b complex with the proteins Ioc2 and Ioc4 (Vary et al., 2003). Furthermore, Isw1 has a role independent of either complex in regulating transcriptional silencing at the ribosomal DNA locus in *S. cerevisiae* (Mueller and Bryk, 2007). It will be interesting to examine whether the absence of either Isw1 or the Isw1a chromatin remodeling complex results in DNA damage or whether these proteins are involved in sensing DNA damage. Alternatively, mutations in these genes might indirectly affect genome integrity by affecting the transcription of one/more DNA damage sensors or DNA repair proteins.

A particularly strong interaction observed was with the Swr1 complex which is involved in replacement of chromatin-bound H2A with the histone variant H2A.Z (Krogan et al., 2003). This complex is highly conserved and has roles in transcription (Mizuguchi et al., 2004) and is proposed to be required for non-homologous end-joining DNA repair (van Attikum et al., 2007). In this screen, mutations in the Swr1 complex strongly interacted with the *mrc1* mutation. Mrc1 is important for normal replication (Katou et al., 2003; Osborn and Elledge, 2003; Szyjka et al., 2005), sister chromatid cohesion (Xu et al., 2007; Xu et al., 2004), and the replication checkpoint (Alcasabas et al., 2001). The *mrc1-aq* allele is a separation-of-function allele, which is deficient

specifically in the checkpoint role of *MRC1*. The Swr1 complex mutations did not cause increased GCR scores in combination with *mrc1-aq*, indicating that a checkpoint-independent role of MRC1 is important to suppress genome instability in cells lacking a functional Swr1 complex. Further studies are required to examine whether the Swr1 complex is directly involved in creating or sensing/repairing DSBs or whether it acts indirectly via its effects on gene transcription.

In addition to the novel results discussed above, the screen revealed some interactions that were consistent with previous studies. For instance, the *mec1 tel1* double mutant had a very high GCR patch score (3.33), which was greater than the score of either single mutant (*mec1*: 1.89 and *tel1*: 1.17). This result is consistent with previous studies showing that Mec1 and Tel1 have redundant roles in suppressing the formation of GCRs mediated by unique sequences (Myung et al., 2001) and reveals that these genes are also functionally redundant in suppressing duplication-mediated GCRs. The elevated GCR score of the replication checkpoint-related mutant strains (*mrc1* and *tof1*) is also consistent with previous studies showing that these genes are important for preventing duplication-mediated GCRs (Putnam et al., 2009a).

In conclusion, this project has identified a plethora of novel candidate complexes and pathways that are required to maintain genome stability in the absence of a normal checkpoint response. These observations have highlighted multiple avenues for further mechanistic studies to elucidate the roles of individual complexes or pathways in preventing GCR formation such as introducing functional mutations or using genes that interacted with checkpoints as new queries for a similar screen. Such studies will also be useful to inform analysis of cancer genome sequencing data and might prove invaluable

in identifying previously unknown genes and pathways that are involved in cancer-related genome instability.

This work in part includes material currently being prepared for publication: Putnam, Chris; Bell, Sara; Srivatsan, Anjana; Martinez, Sandra; Nene, Rahul; and Clotfelter, Sarah.

FIGURES

A

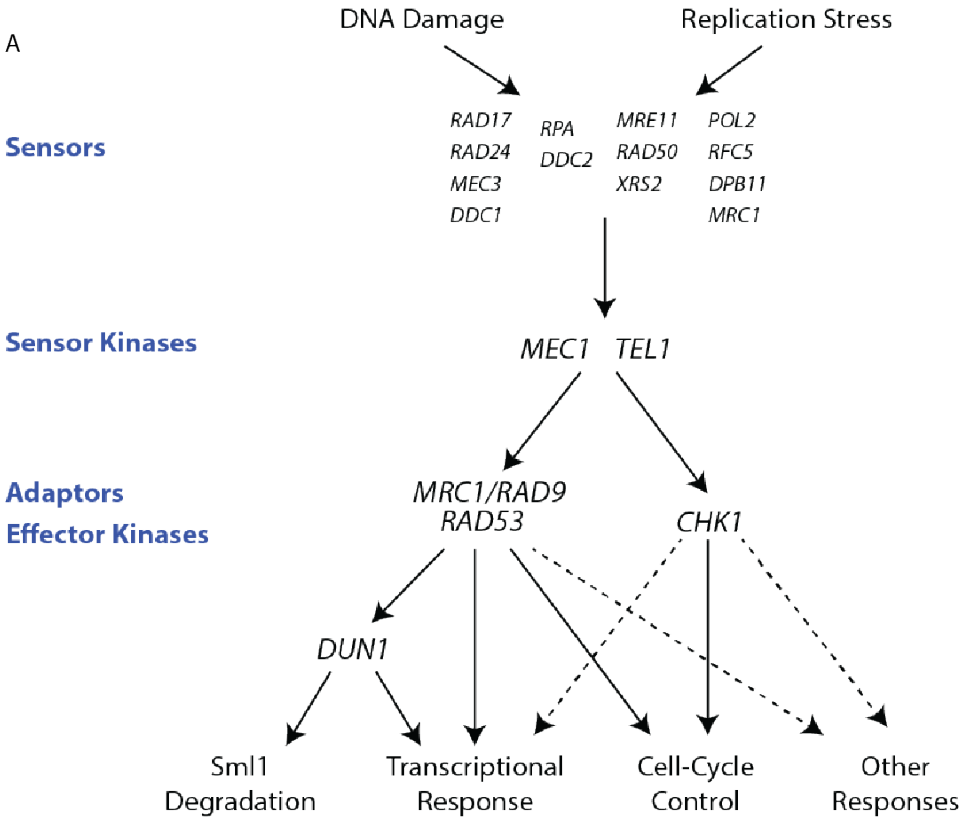


B

| Class | *S. cerevisiae* | *H. sapiens* |
|---|---|---|
| Sensors | MEC1 | ATR |
| | RAD17 | RAD1 |
| Adaptors | RAD9 | 53BP1 |
| | MRC1 | CLSPN |
| Effector kinases | CHK1 | CHK1 |
| | RAD53 | CHK2 |
| | DUN1 | |

**Figure 1: Checkpoint Pathway and Homologs.** A. Simplified checkpoint pathway beginning with DNA damage or replication stress being sensed leading to phosphorylation cascade by kinases leading to cell responses. B. List of the checkpoint genes chosen for this study and their human homologs.

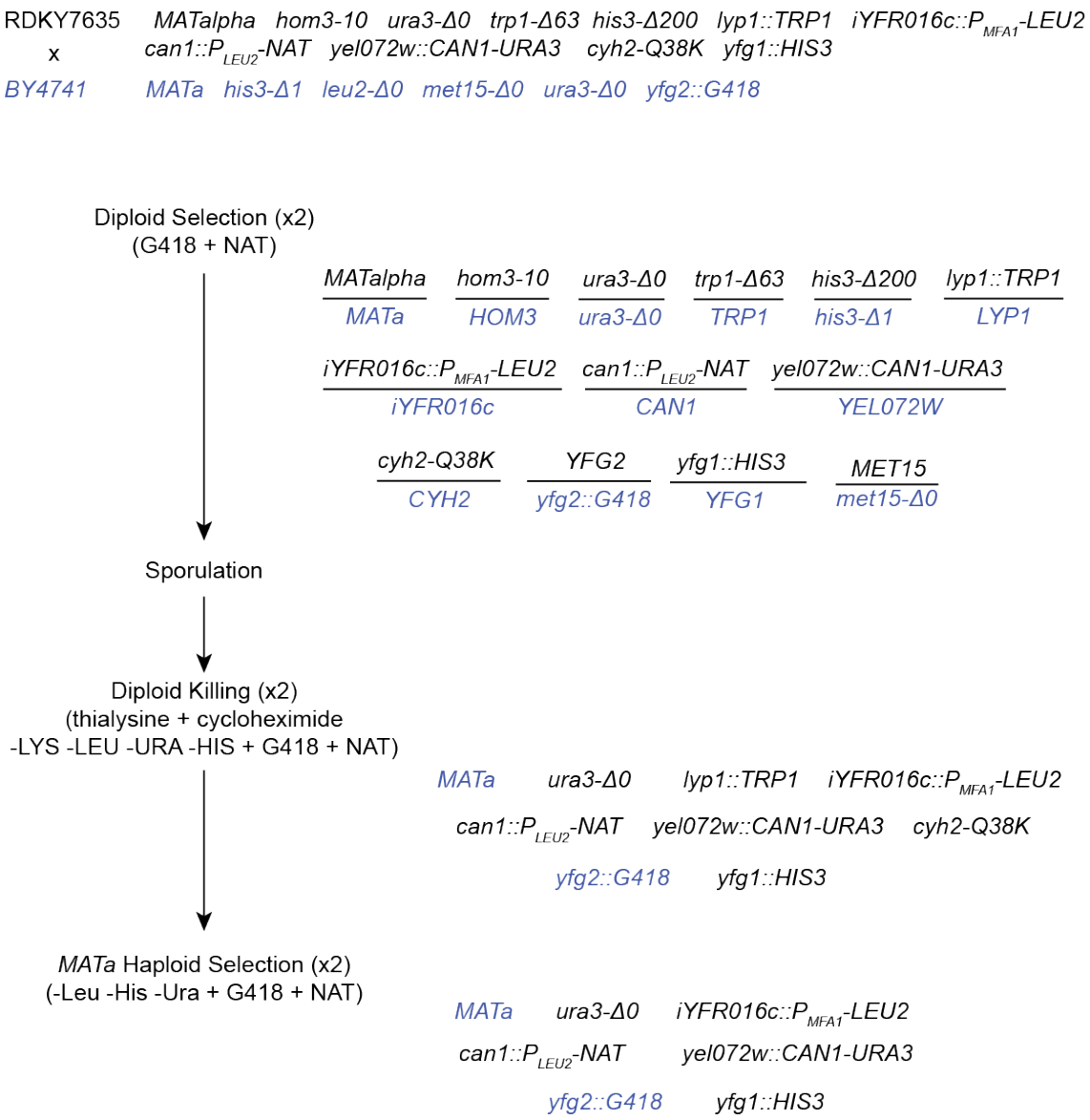


**Figure 2: Systematic Crosses Flow Chart.** The strain RDKY7635 and its derivatives were crossed to a deletion collection using a RoToR (Singer) robot. The strains were first mated, then plated on Diploid Selection Media, Sporulation Media, Diploid Killing Media, and finally Haploid Selection Media in order to obtain the genetic markers at each step shown right of the flow chart. More details in Materials and Methods section as well as in Results.

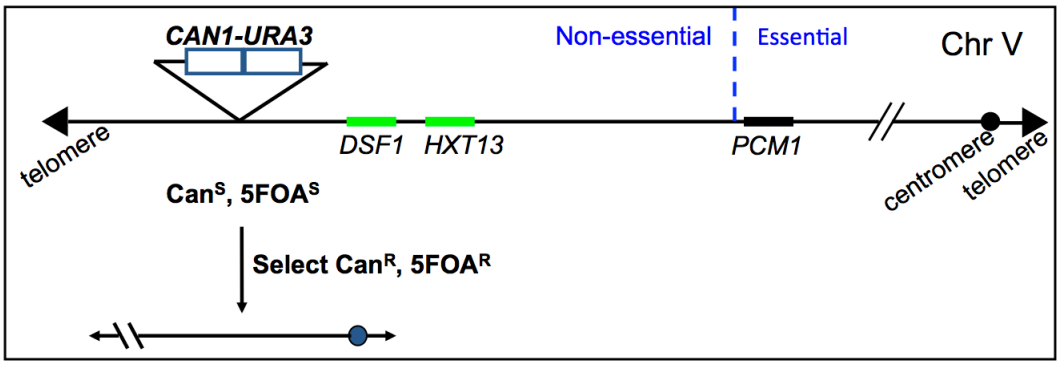


**Regions with imperfect homology to *DSF1/ HXT13*:**

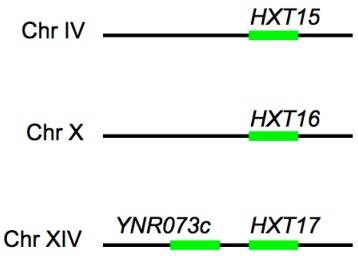


**Figure 3: dGCR Assay.** *CAN1-URA3* cassette inserted into the left arm of chromosome V. *PCM1* is the last essential gene. DSF1 and HXT13 have regions of imperfect homology with chromosomes IV, X, and XIV.

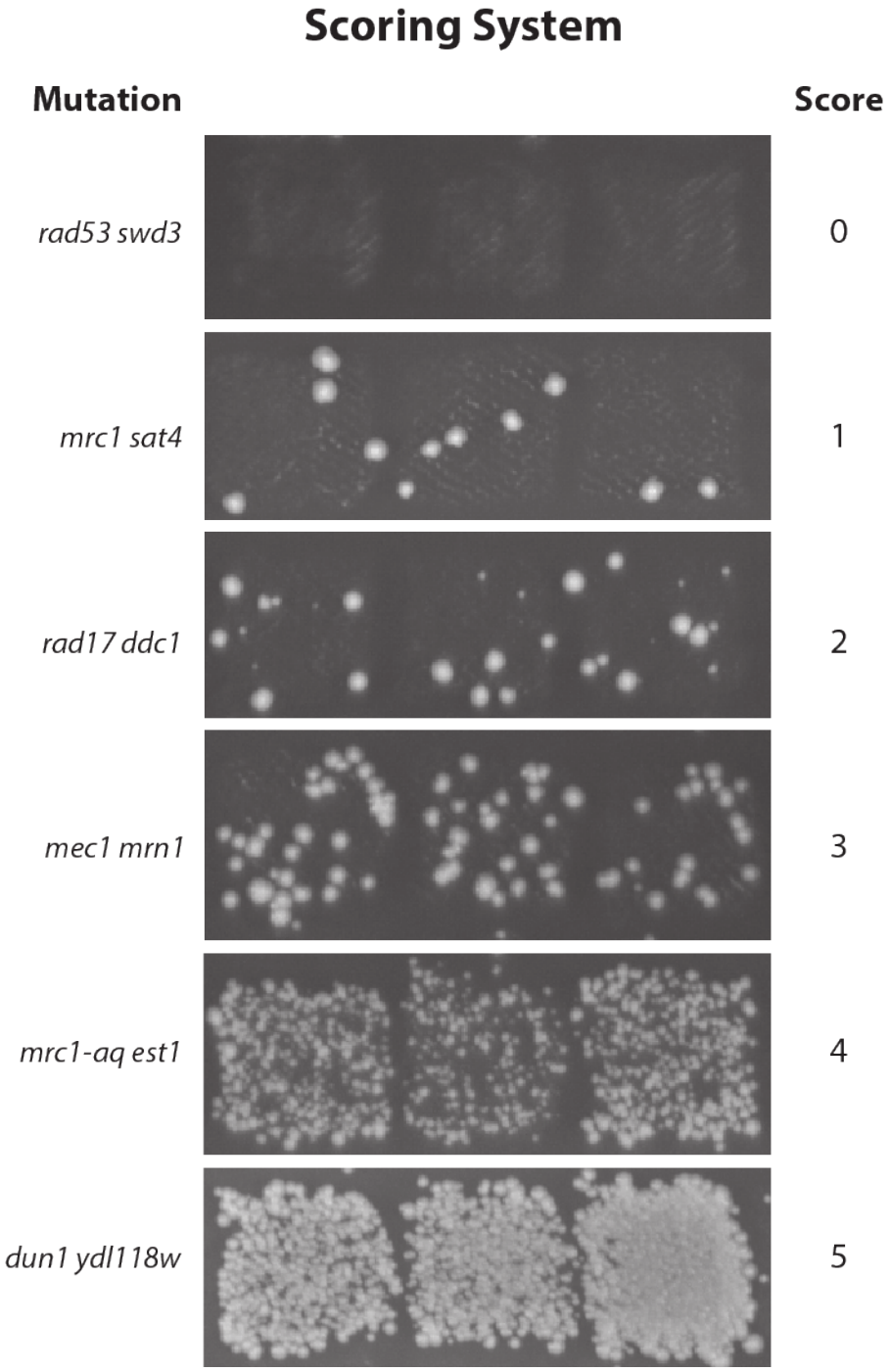


**Figure 4: Patch scoring system.** Patches were scored based on the number of papillae formed on Canavanine 5-FOA plates.

A

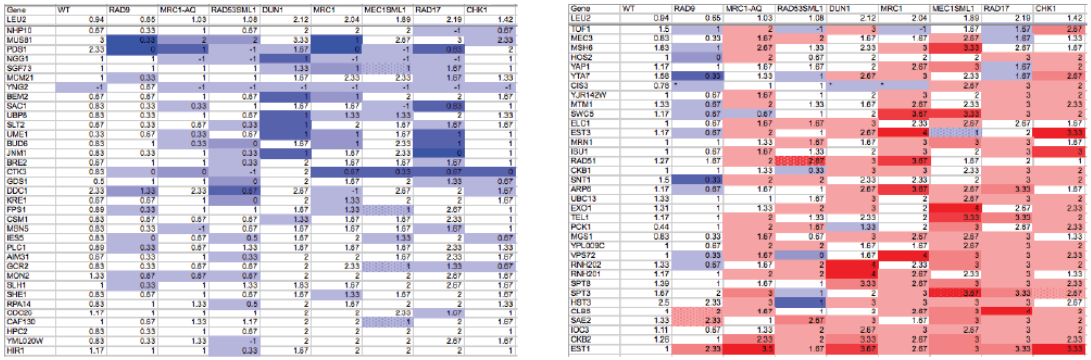

B

| Gene | WT | RAD9 | MRC1-AQ | RAD53SML1 | DUN1 | MRC1 | MEC1SML1 | RAD17 | CHK1 |
|---|---|---|---|---|---|---|---|---|---|
| *LEU2* | 0.94 | 0.65 | 1.03 | 1.08 | 2.12 | 2.04 | 1.89 | 2.19 | 1.42 |
| *CKB1* | 1 | 1 | 1.33 | 0.33 | 3 | 3 | 2.33 | 3 | 2 |
| *CKB2* | 1.26 | 1 | 2.33 | 2 | 3.33 | 2.67 | 3 | 3 | 2.33 |
| *IOC3* | 1.11 | 0.67 | 1.33 | 2 | 2.67 | 3 | 2.67 | 3 | 2 |
| *ISW1* | 1 | 1 | 0.67 | 0.33 | 3 | 2.67 | 2 | 2.67 | 1.33 |
| *RNH201* | 1.17 | 1 | 2 | 2 | 4 | 2.67 | 2.33 | 3 | 1.33 |
| *RNH202* | 1.33 | 0.67 | 1.67 | 2 | 4 | 2.33 | 3 | 3 | 2 |
| *RNH203* | 1.67 | 1 | 2 | -1 | 4 | 2.33 | 2.67 | 3 | 2 |
| *TEL1* | 1.17 | 1 | 2 | 1.33 | 2.33 | 2 | 3.33 | 3.33 | 2 |
| *YKU70* | 1.33 | 1 | 1.17 | 1.33 | 3.67 | 2 | 2 | 3 | 1.33 |
| *YKU80* | 1.67 | 0.67 | 1.33 | 1 | 3.67 | 2 | 2 | 3 | 2 |
| *EST3* | 1.17 | 0.67 | 2 | 1 | 2.67 | 4 | 1 | 2 | 3.33 |
| *EST1* | 1 | 2.33 | 3.5 | 1.67 | 3.67 | 2.67 | 3 | 3.33 | 3.33 |
| *RIF2* | 0.83 | 0.67 | 1 | 1.67 | 2 | 2 | 1.33 | 2.67 | 1.67 |
| *ARP6* | 1.17 | 0.67 | 1.67 | 1 | 2.67 | 3.67 | 2.67 | 3.33 | 1.67 |
| *VPS72* | 1 | 0.33 | 1.67 | 0 | 1.67 | 4 | 3 | 3 | 2.33 |
| *VPS71* | 1 | 0.33 | 1 | 0 | 2 | 3.33 | 2.33 | 3 | 1.33 |
| *SWR1* | 1.3 | 0.67 | 1 | 0 | 2 | 4 | 3 | 2.33 | 1.67 |
| *SWC5* | 1.17 | 0.67 | 0.67 | 1 | 2 | 3.67 | 3.33 | 3 | 2 |
| *HTZ1* | 0.67 | -2 | 0.67 | 1 | 2 | 2 | 3.67 | 3 | 1.33 |
| *SWC3* | 0.83 | 0.67 | 1.33 | 0 | 2 | 4 | 2.67 | 2.33 | 2 |
| *YAF9* | 0.83 | 1 | 0.33 | 1 | 2 | 2 | 2.33 | 2.33 | 2 |


**Figure 5: Candidate interacting complexes.** A. Samples of average score spreadsheet with low interacting genes with checkpoints (left) as well as high interactions (right). B. High interacting complexes or clusters based on function.

TABLES

**Table 1: Average doubling times of checkpoint mutants.**

| Query | Avg. Doubling Time (min)* |
|---|---|
| Ctrl | 99 [1.1] |
| *rad17* | 98 [1.3] |
| *mrc1* | 109 [1.3] |
| *mrc1-aq* | 92 [1.4] |
| *mec1sml1* | 100 [1.2] |
| *sml1* | 92 [0.6] |
| *rad53sml1* | 136 [6.9] |
| *rad9* | 99 [2.4] |
| *dun1* | 104 [5.0] |
| *chk1* | 99 [3.0] |

*Standard deviations shown in brackets.

**Table 2: GCR rates for select double mutants**

| | Rate | | | |
|---|---|---|---|---|
| **Strain** | WT | *mec1* | *rad17* | *mrc1* |
| **RDKY #** | 7635 | 8045 | 8049 | 7636 |
| *leu2* CTRL | *8.6 [4.7-13] × $10^{-8}$ (1) | *5.6 [2.5-7.2] × $10^{-7}$ (6.5) | *5.7 [3.6-7.5] × $10^{-7}$ (6.6) | *3.1 [1.4-6.8] × $10^{-7}$ (3.6) |
| *spt8* | *7.3 [4.8-12] × $10^{-7}$ (8.5) | 8.4 [6.0-32] × $10^{-7}$ (9.8) | 6.5 [5.6-7.9] × $10^{-7}$ (7.5) | ND |
| *ckb2* | *3.92 [3.1-4.2] × $10^{-7}$ (4.6) | 9.1 [4.6-12] × $10^{-7}$ (11) | ND | ND |
| *rnh202* | *1.85 [1.1-9.0] × $10^{-7}$ (2.2) | 6.9 [3.6-9.2] × $10^{-7}$ (8.1) | 7.5 [4.4-18] × $10^{-7}$ (8.7) | |
| *tel1* | *3.38 [2.0-4.9] × $10^{-7}$ (4.0) | | 10.0 [7.8-14] × $10^{-7}$ (12) | 2.87 [1.5-6.1] × $10^{-7}$ (3.3) |
| *yku70* | *6.70 [3.9-1.9] × $10^{-8}$ (0.78) | 3.5 [2.8-4.1] × $10^{-7}$ (4.1) | 1.8 [9.5-30] × $10^{-6}$ (20) | 8.0 [4.2-12] × $10^{-7}$ (9.3) |

**Rate of accumulating $Can^r$ 5-$FOA^r$ progeny. The number in parentheses is the fold increase relative to the standard wild-type rate (8.59 × $10^{-8}$). Numbers in brackets are the 95% confidence interval limits

* Rates previously measured in the Kolodner lab.

ND – Not determined.

**Table 3: Ploidy of select double mutant strains.** Ploidy determined by flow cytometry. H represents Haploid, D represents Diploid, and x indicates strains that were not tested.

| | ckb1 | ckb2 | rnh201 | rnh202 | rnh203 | tel1 | yku70 | yku80 | dnl4 | clb5 | cln2 | mgs1 | idh2 | ubc13 | mms2 |
|---|---|---|---|---|---|---|---|---|---|---|---|---|---|---|---|
| **WT** | H | H | H | H | H | H | H | H | H | H | H | H | H | H | H |
| **mec1** | H | H | H | H | H | H | H | H | H | H | H | H | H | H | H |
| **rad17** | H | H | H | H | H | H | H | H | H | H | H | H | H | H | H |
| **rad9** | H | H | H | H | H | H | H | H | H | H | H | H | H | H | H |
| **mrc1** | H | H | H | H | H | H | H | H | H | H | H | x | H | H | H |
| **mrc1-aq** | H | H | H | H | H | H | H | H | H | H | H | H | H | H | H |
| **chk1** | H | H | H | H | H | H | H | H | H | H | H | H | H | H | H |
| **rad53** | D | D | H | H | x | H | H | H | H | D | H | H | H | H | H |
| **dun1** | H | H | H | H | H | H | H | H | H | D | D | H | H + D | H | H |

**Table 4: List of Candidate Complexes and Pathways that Interact with Checkpoints to Suppress GCRs**. List generated based on average patch scores as well as criteria described in previously in Results.

| |
|---|
| **DNA Repair & DNA Damage Response** |
| Mitotic homologous recombination |
| Post replication repair |
| Cul8-RING ubiquitin ligase complex |
| Replication checkpoint & replication proteins |
| Mismatch repair |
| RNase H2 |
| Telomere maintenance |
| DNA damage checkpoint |
| **Histone Modification & Transcription** |
| Swr1 complex |
| Oxidative stress response |
| Telomere silencing |
| Set3C histone deacetylase |
| Isw1a chromatin remodeling complex |
| RNA polymerase I & II transcription |
| mRNA processing |
| Rpd3L complex |
| **Other** |
| Casein kinase II |
| Cell cycle progression |
| NatA N-terminal acetyltransferase |
| Iron sulfur cluster biosynthesis |

**Table 5: Average GCR Scores for 20 Double Mutant Complexes.** Darkness of red indicates increase in GCR scores compared to the higher of the two single mutants; darkness of blue indicates decrease in GCR scores compared to the higher of the two single mutants. Black boxes indicate the strains did not grow. Black boxes with a * indicate strains that were not crossed.

| Gene | *WT* | *RAD9* | *MRC1-AQ* | *RAD53 SML1* | *DUN1* | *MRC1* | *MEC1 SML1* | *RAD17* | *CHK1* |
|---|---|---|---|---|---|---|---|---|---|
| ***LEU2*** | **0.94** | **0.65** | **1.03** | **1.08** | **2.12** | **2.04** | **1.89** | **2.19** | **1.42** |
| Mitotic Homologous Recombination | | | | | | | | | |
| *RAD51* | 1.27 | 1.67 | 2 | 2.67 | 3 | 3.67 | 1.67 | 2 | 1 |
| *RAD59* | 1.02 | 0.33 | 0.67 | 0.67 | 2.67 | 1 | 2.33 | -1 | 2 |
| *RAD55* | 0.67 | 0.67 | 1.67 | 1 | 2.67 | 0.33 | 2 | 1.67 | 1 |
| *RAD57* | 1.17 | 0.67 | 1 | 1 | 3 | 1 | 2.33 | 1.33 | 1 |
| *EXO1* | 1.31 | 1 | 1.33 | 2 | 3 | 2 | 4 | 2.67 | 2.33 |
| *RDH54* | 1 | 0.33 | 1.33 | 1.67 | 0.67 | 2 | 3 | 3 | 1 |
| *MGS1* | 0.83 | 0.33 | 1.67 | 0.67 | 3 | 2.67 | 2.67 | 3 | 1.33 |
| *RAD52* | 1 | 1.33 | 0.33 | 1.33 | 1 | 1.33 | 1.33 | 0.33 | 1 |
| *RAD54* | 0.83 | 1 | 0 | 1.67 | 2.33 | 0.67 | 2 | | 1.67 |
| *SAE2* | 1.33 | 2.33 | 1 | 2.67 | 3 | 1.67 | 3 | 3 | 2 |
| | | | | | | | | | |
| Post Replication Repair | | | | | | | | | |
| *UBC13* | 1.33 | 1 | 1 | 1.67 | 3 | 2 | 2.67 | 3 | 2 |
| *MMS2* | 1.5 | 1 | 1 | 1.67 | 3 | 2 | 2 | 3 | 2 |
| *RAD5* | 3.83 | 1.67 | 3.33 | 2 | 4 | 3.33 | 3 | 3 | 3 |
| *RAD6* | 2.33 | 1.67 | 2.67 | 2.33 | 3.67 | 2.33 | 2 | 3.33 | 1.67 |
| *RAD18* | 3.81 | 1 | 3 | 1.67 | 4 | 3 | 3 | 2.67 | 3 |
| *REV3* | 1.22 | 1 | 2 | 1.33 | 3 | 2 | 2.33 | 3 | 1.67 |
| *REV7* | 1.33 | 1 | 2 | 1 | 2.33 | 2.33 | 2.33 | 3 | 1 |
| *REV1* | 1 | 1.33 | 2 | 1 | 2.33 | 2.33 | 2.33 | 2.33 | 1.33 |
| *RAD30* | 1 | 0.33 | 2 | 1 | 2.33 | 2 | 2 | 2 | 1 |
| | | | | | | | | | |
| Cul8-RING ubiquitin ligase complex | | | | | | | | | |
| *RTT101* | 1.5 | 1.33 | 1.33 | 1 | 2.67 | 2 | 2 | 3 | 2 |
| *RTT107* | 1.7 | 0.67 | 1.33 | 0.67 | 2.33 | 1.33 | 2.33 | 2.67 | 1.67 |
| *MMS22* | 1 | 2 | 1 | 1 | 1.67 | 1 | 1.67 | 1 | 1.67 |
| *MMS1* | 1.67 | 2 | 1.33 | 1.33 | 2 | 2 | 2.33 | 2 | 2.67 |
| | | | | | | | | | |

**Table 5: Continued**

| Gene | *WT* | *RAD9* | *MRC1-AQ* | *RAD53 SML1* | *DUN1* | *MRC1* | *MEC1 SML1* | *RAD17* | *CHK1* |
|---|---|---|---|---|---|---|---|---|---|
| ***LEU2*** | **0.94** | **0.65** | **1.03** | **1.08** | **2.12** | **2.04** | **1.89** | **2.19** | **1.42** |
| Replication checkpoint & replication proteins | | | | | | | | | |
| *FOB1* | 0.67 | 0 | 1.33 | 1.33 | 2.67 | 2 | 2.67 | 2.33 | 1.67 |
| *DPB3* | 0.83 | 1 | 1.33 | 1.33 | 2.33 | 3 | 2.33 | 2.67 | 2 |
| *DPB4* | 1.33 | 1 | 1.33 | 1 | 3.33 | 3 | 2 | 2.33 | 1.33 |
| *TOF1* | 1.5 | 1 | 2 | | 3 | | 1.67 | 1.67 | 2.67 |
| *CSM3* | 1.83 | 1 | 1.67 | 1 | 3 | 3 | 2 | 1.67 | 1.67 |
| *MRC1* | 2.04 | 1.33 | 0.67 | 1.67 | 2 | 2 | 1 | | 2 |
| *RAD27* | 3.5 | 3 | 3 | 1 | 3.67 | 1 | | | 4 |
| | | | | | | | | | |
| Mismatch repair | | | | | | | | | |
| *MSH6* | 1.83 | 1 | 2.67 | 1.33 | 2.33 | 3 | 3.33 | 2.67 | 1.67 |
| *MSH3* | 1 | 0.67 | 0.33 | 1.33 | 1.33 | 2 | 2 | 1.67 | 1 |
| *PMS1* | 1.17 | 1.67 | 1.33 | 2 | 1.67 | 2.33 | 2 | 3 | 1 |
| *MLH3* | 1.33 | 0.33 | 1 | 2.67 | 1.67 | 2.67 | 2 | 2 | 1 |
| *MLH1* | 2 | 1 | 1.33 | 2 | 1.67 | 2.67 | 2.33 | 2 | 1.67 |
| | | | | | | | | | |
| RNase H2 | | | | | | | | | |
| *RNH201* | 1.17 | 1 | 2 | 2 | 4 | 2.67 | 2.33 | 3 | 1.33 |
| *RNH202* | 1.33 | 0.67 | 1.67 | 2 | 4 | 2.33 | 3 | 3 | 2 |
| *RNH203* | 1.67 | 1 | 2 | | 4 | 2.33 | 2.67 | 3 | 2 |
| | | | | | | | | | |
| Telomere Maintenance | | | | | | | | | |
| *TEL1* | 1.17 | 1 | 2 | 1.33 | 2.33 | 2 | 3.33 | 3.33 | 2 |
| *YKU70* | 1.33 | 1 | 1.17 | 1.33 | 3.67 | 2 | 2 | 3 | 1.33 |
| *YKU80* | 1.67 | 0.67 | 1.33 | 1 | 3.67 | 2 | 2 | 3 | 2 |
| *EST3* | 1.17 | 0.67 | 2 | 1 | 2.67 | 4 | 1 | 2 | 3.33 |
| *EST1* | 1 | 2.33 | 3.5 | 1.67 | 3.67 | 2.67 | 3 | 3.33 | 3.33 |
| *RIF2* | 0.83 | 0.67 | 1 | 1.67 | 2 | 2 | 1.33 | 2.67 | 1.67 |
| | | | | | | | | | |
| Swr1 Complex | | | | | | | | | |
| *ARP6* | 1.17 | 0.67 | 1.67 | 1 | 2.67 | 3.67 | 2.67 | 3.33 | 1.67 |
| *VPS72* | 1 | 0.33 | 1.67 | 0 | 1.67 | 4 | 3 | 3 | 2.33 |
| *VPS71* | 1 | 0.33 | 1 | 0 | 2 | 3.33 | 2.33 | 3 | 1.33 |
| *SWR1* | 1.3 | 0.67 | 1 | 0 | 2 | 4 | 3 | 2.33 | 1.67 |
| *SWC5* | 1.17 | 0.67 | 0.67 | 1 | 2 | 3.67 | 3.33 | 3 | 2 |
| *HTZ1* | 0.67 | | 0.67 | 1 | 2 | 2 | 3.67 | 3 | 1.33 |
| *SWC3* | 0.83 | 0.67 | 1.33 | 0 | 2 | 4 | 2.67 | 2.33 | 2 |
| *YAF9* | 0.83 | 1 | 0.33 | 1 | 2 | 2 | 2.33 | 2.33 | 2 |
| | | | | | | | | | |

**Table 5: Continued**

| Gene | *WT* | *RAD9* | *MRC1-AQ* | *RAD53 SML1* | *DUN1* | *MRC1* | *MEC1 SML1* | *RAD17* | *CHK1* |
|---|---|---|---|---|---|---|---|---|---|
| ***LEU2*** | **0.94** | **0.65** | **1.03** | **1.08** | **2.12** | **2.04** | **1.89** | **2.19** | **1.42** |
| DNA Damage Checkpoint | | | | | | | | | |
| *MEC3* | 0.83 | 0.33 | 1.67 | 2 | 1.67 | 1.67 | 2.67 | 1.67 | 1.33 |
| *DDC1* | 2.33 | 1.33 | 2.33 | 0.67 | 2.67 | | 2.67 | 2 | 1.67 |
| *RAD17* | 2.19 | 2 | 3 | 2.67 | 1.67 | 1 | 3 | | 1.67 |
| *SML1* | 1 | 0.67 | 1 | 2 | 1.67 | 1.33 | 2.67 | 2.67 | 0.33 |
| *MEC1 SML1* | 1.89 | 1.33 | 2 | 1.33 | 2 | 0 | | 3 | 1.33 |
| *DDC2 SML1* | 2 | 1.67 | 1.33 | 1.67 | 1.67 | 1.33 | 1.67 | 3 | 1 |
| *RAD53SML1* | 1.08 | 1.67 | 0.67 | | 0.67 | 1 | 2.33 | 1.67 | 1 |
| *RAD53-21* | 1 | 0.67 | 2.67 | | | 1 | 2.33 | 1.83 | 1 |
| *CHK1* | 1.42 | 0.67 | 3 | 1.67 | 1.67 | 2.33 | 2 | 2.67 | |
| *PDS1* | 2.33 | 0 | 1 | | 1.67 | 0 | | 0.83 | 2 |
| *ELG1* | 2.17 | 1 | 3.67 | 1.33 | 2 | 5 | 2.67 | 2.67 | 1.67 |
| *RAD24* | 2.17 | 2 | 2 | 2 | 2 | | 2 | 2.67 | 2 |
| | | | | | | | | | |
| Casein Kinase II | | | | | | | | | |
| *CKB1* | 1 | 1 | 1.33 | 0.33 | 3 | 3 | 2.33 | 3 | 2 |
| *CKB2* | 1.26 | 1 | 2.33 | 2 | 3.33 | 2.67 | 3 | 3 | 2.33 |
| | | | | | | | | | |
| Oxidative Stress Response | | | | | | | | | |
| *SKN7* | 1.83 | 1 | 1.67 | 1.67 | 2.33 | 2 | 3 | 3 | 2 |
| *YAP1* | 1.17 | 1 | 1.67 | 1.67 | 2 | 2.67 | 3 | 1.67 | 2 |
| *ALO1* | 0.83 | 0.67 | 1.33 | 1.33 | 2 | 2 | 3 | 3 | 1 |
| | | | | | | | | | |
| Telomere Silencing | | | | | | | | | |
| *ESC1* | 1 | 0.67 | 1.67 | 2 | 2 | 2 | 2 | 3 | 1.67 |
| *DOT1* | 0.33 | 1 | 1 | 1.33 | 1.33 | 4 | 2.67 | 3 | 1 |
| *DOT6* | 0.83 | 0.5 | 1 | 2 | 2 | 1.67 | 1.67 | 2.67 | 1.33 |
| *SPT21* | 1 | 1 | 1.33 | 1 | 2.33 | 3 | 1.33 | 1.33 | 1.33 |
| *NPT1* | 0.5 | 0.67 | 1 | 1 | 1 | 2.67 | 2 | 1.67 | 1 |
| *HST3* | 2.5 | 2.33 | 3 | 1 | 3 | 3 | 3 | 3 | 2.67 |
| *HST4* | 1 | 1 | 1 | 1 | 2 | 2.33 | 1.67 | 2 | 1 |
| | | | | | | | | | |
| NatA N-Terminal Acetyltransferase | | | | | | | | | |
| *ARD1* | 1 | 1 | 1.67 | 1.33 | 1.33 | 1.67 | 3 | 4 | 1.67 |
| *NAT1* | 0.83 | 0.67 | 0.67 | 1.67 | 0.67 | 1.67 | 2 | 1.67 | 1 |
| | | | | | | | | | |
| Set3C Histone Deacetylase | | | | | | | | | |
| *SNT1* | 1.5 | 0.33 | 2 | 2 | 2.33 | 2.33 | 2 | 3 | 2 |
| *SIF2* | 1.17 | 0.33 | 1.33 | 1.33 | 3 | 2 | 2.33 | 3 | 1.67 |
| *HOS2* | 1 | 0 | 2 | 0.67 | 2 | 2 | 2 | 3 | 2 |

**Table 5: Continued**

| Gene | *WT* | *RAD9* | *MRC1-AQ* | *RAD53 SML1* | *DUN1* | *MRC1* | *MEC1 SML1* | *RAD17* | *CHK1* |
|---|---|---|---|---|---|---|---|---|---|
| ***LEU2*** | **0.94** | **0.65** | **1.03** | **1.08** | **2.12** | **2.04** | **1.89** | **2.19** | **1.42** |
| Isw1a complex | | | | | | | | | |
| *IOC3* | 1.11 | 0.67 | 1.33 | 2 | 2.67 | 3 | 2.67 | 3 | 2 |
| *ISW1* | 1 | 1 | 0.67 | 0.33 | 3 | 2.67 | 2 | 2.67 | 1.33 |
| | | | | | | | | | |
| Cell Cycle Progression | | | | | | | | | |
| *WHI5* | 0.67 | 1 | | 1.33 | 3 | 0.67 | | | 2 |
| *CLB5* | 1 | 2 | 1.67 | 1 | 2 | 2.67 | 3 | 4 | 2 |
| *CLN2* | 0.67 | 1 | 1 | 1.67 | 1.33 | 2 | 2.67 | 3 | 1 |
| *SWI6* | 1 | 1 | 1 | 0.33 | 0.67 | 2.33 | 1 | 3 | 1.33 |
| *MBP1* | 1 | 1 | 0.67 | 1 | 2.67 | 1 | 2.67 | 2 | 1.33 |
| | | | | | | | | | |
| RNA polymerase I & II transcription | | | | | | | | | |
| *RTT103* | 0.83 | 1.33 | 0.67 | 0.67 | 2.67 | 2 | 2 | 3 | 1 |
| *DST1* | 1.67 | 1 | 1.67 | 1.33 | 2.33 | 2 | 3 | 2.67 | 2 |
| *SIN4* | 1 | 1 | 1.33 | 1.67 | 2 | 2 | 2.67 | 3 | 1.33 |
| *MED1* | 0.67 | 0.33 | 1 | 1.33 | 2 | 2.67 | 2.67 | 1.67 | 1.33 |
| *NUT1* | 0.83 | 0.67 | 1.33 | 1 | 2 | 2 | 3 | 2.33 | 1.67 |
| *RPA34* | 0.83 | 1 | 1 | 1 | 2.67 | 1.67 | 2.67 | 3 | 1.67 |
| *RPA14* | 0.83 | 1 | 1.33 | 0.5 | 2 | 1.67 | 2 | 2 | 1.33 |
| *ELC1* | 1 | 0.67 | 1.67 | 1.67 | 3 | 2.33 | 2.67 | 2.67 | 1.67 |
| *SFL1* | 1.11 | * | 1.67 | 1 | * | * | 2.67 | 3 | 1.67 |
| | | | | | | | | | |
| mRNA processing | | | | | | | | | |
| *PAT1* | 0.83 | 0.33 | 0.33 | | 1 | 2 | 1.67 | 1.67 | 2 |
| *SLF1* | | 0.33 | 1.33 | 2 | 2.33 | 2 | 2.33 | 2.67 | 1.67 |
| *SRO9* | 1.17 | 0.67 | 1.33 | 1.33 | 2 | 3 | 2 | 3 | 1.33 |
| *YPL009C* | 1 | 0.67 | 2 | 2 | 1.67 | 1.67 | 2.67 | 3 | 2 |
| *LSM6* | 1.17 | 0 | 1.33 | 1.33 | 1 | 1.67 | 2.67 | 3 | 1.33 |
| *PUB1* | 0.67 | 0.17 | 1.67 | 2 | 1.17 | 1.33 | 2.67 | 2.33 | 1.67 |
| *GBP2* | 1.17 | 0.67 | 1.67 | 1.67 | 2 | 2 | 1 | 2 | 2 |
| *EDC3* | 1.22 | * | 1 | 1.33 | * | * | 2 | 2.33 | 2 |
| | | | | | | | | | |
| Iron sulfur cluster biosynthesis | | | | | | | | | |
| *ISU1* | 1 | 0.67 | 1.67 | 1.33 | 2 | 3 | 2 | 3 | 3 |
| *MET18* | 1.17 | 1.67 | 3 | 0.67 | 1 | 2 | | 0.33 | 1 |

**Table 5: Continued**

| Gene | *WT* | *RAD9* | *MRC1-AQ* | *RAD53 SML1* | *DUN1* | *MRC1* | *MEC1 SML1* | *RAD17* | *CHK1* |
|---|---|---|---|---|---|---|---|---|---|
| ***LEU2*** | **0.94** | **0.65** | **1.03** | **1.08** | **2.12** | **2.04** | **1.89** | **2.19** | **1.42** |
| Rpd3L complex | | | | | | | | | |
| *CTI6* | 1 | 0.33 | 0.67 | 2 | 2 | 1.67 | 2.33 | 1.33 | 0.67 |
| *DEP1* | 0.17 | 0.33 | | 2 | 0.67 | 1.67 | 2 | 1 | 1 |
| *RXT2* | 1.17 | 0.67 | 0.67 | 2 | 1 | 1 | 2.67 | 0.67 | 0.67 |
| *UME6* | 1 | 0.67 | | 0.67 | 0 | 2 | | 1.67 | 1 |
| *SDS3* | 0.67 | 1 | 0.67 | 0.67 | 0.33 | 1 | 2.33 | 0.33 | 1 |
| *SAP30* | 0.5 | 0 | 0.67 | 2 | 0.67 | 1 | 2 | 0.33 | 0.67 |
| *PHO23* | 0.83 | 0.67 | 0.67 | 1.67 | 1 | 1.33 | 2 | 2 | 0.67 |
| *RPD3* | 0.17 | 1 | | 1 | 0 | 1.67 | 1 | 2 | 0.33 |
| *SIN3* | 0.33 | 0.67 | | 1.33 | 0.33 | 0.67 | 2.33 | | 0 |
| *UME1* | 0.33 | 0.67 | 0.33 | 0.67 | 1 | 1 | 1.67 | 1 | 1 |

# REFERENCES


Abdel-Rahman, W.M., Katsura, K., Rens, W., Gorman, P.A., Sheer, D., Bicknell, D., Bodmer, W.F., Arends, M.J., Wyllie, A.H., and Edwards, P.A. (2001). Spectral karyotyping suggests additional subsets of colorectal cancers characterized by pattern of chromosome rearrangement. Proceedings of the National Academy of Sciences of the United States of America *98*, 2538-2543.

Ackermann, K., Waxmann, A., Glover, C.V., and Pyerin, W. (2001). Genes targeted by protein kinase CK2: a genome-wide expression array analysis in yeast. Molecular and cellular biochemistry *227*, 59-66.

Alcasabas, A.A., Osborn, A.J., Bachant, J., Hu, F., Werler, P.J., Bousset, K., Furuya, K., Diffley, J.F., Carr, A.M., and Elledge, S.J. (2001). Mrc1 transduces signals of DNA replication stress to activate Rad53. Nature cell biology *3*, 958-965.

Bidwai, A.P., Reed, J.C., and Glover, C.V. (1994). Casein kinase II of Saccharomyces cerevisiae contains two distinct regulatory subunits, beta and beta'. Archives of biochemistry and biophysics *309*, 348-355.

Campbell, P.J., Stephens, P.J., Pleasance, E.D., O'Meara, S., Li, H., Santarius, T., Stebbings, L.A., Leroy, C., Edkins, S., Hardy, C.*, et al.* (2008). Identification of somatically acquired rearrangements in cancer using genome-wide massively parallel paired-end sequencing. Nature genetics *40*, 722-729.

Chen, C., and Kolodner, R.D. (1999). Gross chromosomal rearrangements in Saccharomyces cerevisiae replication and recombination defective mutants. Nature genetics *23*, 81-85.

Chen, S.H., Albuquerque, C.P., Liang, J., Suhandynata, R.T., and Zhou, H. (2010). A proteome-wide analysis of kinase-substrate network in the DNA damage response. The Journal of biological chemistry *285*, 12803-12812.

Davoli, T., Xu, A.W., Mengwasser, K.E., Sack, L.M., Yoon, J.C., Park, P.J., and Elledge, S.J. (2013). Cumulative haploinsufficiency and triplosensitivity drive aneuploidy patterns and shape the cancer genome. Cell *155*, 948-962.

Fouladi, B., Sabatier, L., Miller, D., Pottier, G., and Murnane, J.P. (2000). The relationship between spontaneous telomere loss and chromosome instability in a human tumor cell line. Neoplasia *2*, 540-554.

Ghavidel, A., and Schultz, M.C. (2001). TATA binding protein-associated CK2 transduces DNA damage signals to the RNA polymerase III transcriptional machinery. Cell *106*, 575-584.

Greenman, C., Stephens, P., Smith, R., Dalgliesh, G.L., Hunter, C., Bignell, G., Davies, H., Teague, J., Butler, A., Stevens, C.*, et al.* (2007). Patterns of somatic mutation in human cancer genomes. Nature *446*, 153-158.

Guillemain, G., Ma, E., Mauger, S., Miron, S., Thai, R., Guerois, R., Ochsenbein, F., and Marsolier-Kergoat, M.C. (2007). Mechanisms of checkpoint kinase Rad53 inactivation after a double-strand break in Saccharomyces cerevisiae. Molecular and cellular biology *27*, 3378-3389.

Hanahan, D., and Weinberg, R.A. (2011). Hallmarks of cancer: the next generation. Cell *144*, 646-674.

Harrison, J.C., and Haber, J.E. (2006). Surviving the breakup: the DNA damage checkpoint. Annual review of genetics *40*, 209-235.

Janke, C., Magiera, M.M., Rathfelder, N., Taxis, C., Reber, S., Maekawa, H., Moreno-Borchart, A., Doenges, G., Schwob, E., Schiebel, E.*, et al.* (2004). A versatile toolbox for PCR-based tagging of yeast genes: new fluorescent proteins, more markers and promoter substitution cassettes. Yeast *21*, 947-962.

Katou, Y., Kanoh, Y., Bando, M., Noguchi, H., Tanaka, H., Ashikari, T., Sugimoto, K., and Shirahige, K. (2003). S-phase checkpoint proteins Tof1 and Mrc1 form a stable replication-pausing complex. Nature *424*, 1078-1083.

Kolodner, R.D., Putnam, C.D., and Myung, K. (2002). Maintenance of genome stability in Saccharomyces cerevisiae. Science *297*, 552-557.

Krogan, N.J., Keogh, M.C., Datta, N., Sawa, C., Ryan, O.W., Ding, H., Haw, R.A., Pootoolal, J., Tong, A., Canadien, V.*, et al.* (2003). A Snf2 family ATPase complex required for recruitment of the histone H2A variant Htz1. Molecular cell *12*, 1565-1576.

Landesman-Bollag, E., Romieu-Mourez, R., Song, D.H., Sonenshein, G.E., Cardiff, R.D., and Seldin, D.C. (2001). Protein kinase CK2 in mammary gland tumorigenesis. Oncogene *20*, 3247-3257.

Lea, D.E., and Coulson, C.A. (1949a). The Distribution of the Number of Mutants in Bacterial Populations. Journ of Genetics *49*, 264-285.

Lea, D.E., and Coulson, C.A. (1949b). The distribution of the numbers of mutants in bacterial populations. Journ of Genetics *49*, 264-285.

Lee, S.J., Duong, J.K., and Stern, D.F. (2004). A Ddc2-Rad53 fusion protein can bypass the requirements for RAD9 and MRC1 in Rad53 activation. Molecular biology of the cell *15*, 5443-5455.

Lengauer, C., Kinzler, K.W., and Vogelstein, B. (1998). Genetic instabilities in human cancers. Nature *396*, 643-649.

Lobo, I. (2008). Chromosome Abnormalities and Cancer Cytogenetics. Nature Education *1*.

Loeb, L.A. (2001). A mutator phenotype in cancer. Cancer research *61*, 3230-3239.
Mitelman, F. (1991). Catalog of chromosome aberrations in cancer (New York, New York: Wiley Liss).

Mizuguchi, G., Shen, X., Landry, J., Wu, W.H., Sen, S., and Wu, C. (2004). ATP-driven exchange of histone H2AZ variant catalyzed by SWR1 chromatin remodeling complex. Science *303*, 343-348.

Morris, L.G., Veeriah, S., and Chan, T.A. (2010). Genetic determinants at the interface of cancer and neurodegenerative disease. Oncogene *29*, 3453-3464.

Mueller, J.E., and Bryk, M. (2007). Isw1 acts independently of the Isw1a and Isw1b complexes in regulating transcriptional silencing at the ribosomal DNA locus in Saccharomyces cerevisiae. Journal of molecular biology *371*, 1-10.

Munstermann, U., Fritz, G., Seitz, G., Lu, Y.P., Schneider, H.R., and Issinger, O.G. (1990). Casein kinase II is elevated in solid human tumours and rapidly proliferating non-neoplastic tissue. European journal of biochemistry / FEBS *189*, 251-257.

Myung, K., Datta, A., and Kolodner, R.D. (2001). Suppression of spontaneous chromosomal rearrangements by S phase checkpoint functions in Saccharomyces cerevisiae. Cell *104*, 397-408.

Nowell, P.C., and Hungerford, D.A. (1960). A minute chromosome in human chronic granulocyte leukemia Science *132*.

Osborn, A.J., and Elledge, S.J. (2003). Mrc1 is a replication fork component whose phosphorylation in response to DNA replication stress activates Rad53. Genes & development *17*, 1755-1767.

Padmanabha, R., Chen-Wu, J.L., Hanna, D.E., and Glover, C.V. (1990). Isolation, sequencing, and disruption of the yeast CKA2 gene: casein kinase II is essential for viability in Saccharomyces cerevisiae. Molecular and cellular biology *10*, 4089-4099.

Putnam, C.D., Allen-Soltero, S.R., Martinez, S.L., Chan, J.E., Hayes, T.K., and Kolodner, R.D. (2012). Bioinformatic Identification of genes suppressing genome instability. Proceedings of the National Academy of Sciences of the United States of America *109*, E3251-3259.

Putnam, C.D., Hayes, T.K., and Kolodner, R.D. (2009a). Specific pathways prevent duplication-mediated genome rearrangements. Nature *460*, 984-989.

Putnam, C.D., Jaehnig, E.J., and Kolodner, R.D. (2009b). Perspectives on the DNA damage and replication checkpoint responses in Saccharomyces cerevisiae. DNA repair *8*, 974-982.

Putnam, C.D., and Kolodner, R.D. (2010). Determination of gross chromosomal rearrangement rates. Cold Spring Harbor protocols *2010*, pdb prot5492.

Reid, A.H., Attard, G., Brewer, D., Miranda, S., Riisnaes, R., Clark, J., Hylands, L., Merson, S., Vergis, R., Jameson, C.*, et al.* (2012). Novel, gross chromosomal alterations involving PTEN cooperate with allelic loss in prostate cancer. Modern pathology : an official journal of the United States and Canadian Academy of Pathology, Inc *25*, 902-910.

Rudkin, C.T., Hungerford, D.A., and Nowell, P.C. (1964). DNA Contents of Chromosome Ph1 and Chromosome 21 in Human Chronic Granulocytic Leukemia. Science *144*, 1229-1231.

Saunders, W.S., Shuster, M., Huang, X., Gharaibeh, B., Enyenihi, A.H., Petersen, I., and Gollin, S.M. (2000). Chromosomal instability and cytoskeletal defects in oral cancer cells. Proceedings of the National Academy of Sciences of the United States of America *97*, 303-308.

Sheltzer, J.M., Blank, H.M., Pfau, S.J., Tange, Y., George, B.M., Humpton, T.J., Brito, I.L., Hiraoka, Y., Niwa, O., and Amon, A. (2011). Aneuploidy drives genomic instability in yeast. Science *333*, 1026-1030.

Sikorski, R.S., and Hieter, P. (1989). A system of shuttle vectors and yeast host strains designed for efficient manipulation of DNA in Saccharomyces cerevisiae. Genetics *122*, 19-27.

Smith, S., Hwang, J.Y., Banerjee, S., Majeed, A., Gupta, A., and Myung, K. (2004). Mutator genes for suppression of gross chromosomal rearrangements identified by a genome-wide screening in Saccharomyces cerevisiae. Proceedings of the National Academy of Sciences of the United States of America *101*, 9039-9044.

Solomon, D.A., Kim, T., Diaz-Martinez, L.A., Fair, J., Elkahloun, A.G., Harris, B.T., Toretsky, J.A., Rosenberg, S.A., Shukla, N., Ladanyi, M.*, et al.* (2011). Mutational inactivation of STAG2 causes aneuploidy in human cancer. Science *333*, 1039-1043.

Stephens, P.J., Greenman, C.D., Fu, B., Yang, F., Bignell, G.R., Mudie, L.J., Pleasance, E.D., Lau, K.W., Beare, D., Stebbings, L.A.*, et al.* (2011). Massive genomic rearrangement acquired in a single catastrophic event during cancer development. Cell *144*, 27-40.

Szyjka, S.J., Viggiani, C.J., and Aparicio, O.M. (2005). Mrc1 is required for normal progression of replication forks throughout chromatin in S. cerevisiae. Molecular cell *19*, 691-697.

Toczyski, D.P., Galgoczy, D.J., and Hartwell, L.H. (1997). CDC5 and CKII Control Adaptation to the Yeast DNA Damage Checkpoint. Cell *90*, 1097-1106.

Tong, A.H., and Boone, C. (2006). Synthetic genetic array analysis in Saccharomyces cerevisiae. Methods in molecular biology *313*, 171-192.

Tong, A.H., Evangelista, M., Parsons, A.B., Xu, H., Bader, G.D., Page, N., Robinson, M., Raghibizadeh, S., Hogue, C.W., Bussey, H.*, et al.* (2001). Systematic genetic analysis with ordered arrays of yeast deletion mutants. Science *294*, 2364-2368.

Tong, A.H., Lesage, G., Bader, G.D., Ding, H., Xu, H., Xin, X., Young, J., Berriz, G.F., Brost, R.L., Chang, M.*, et al.* (2004). Global mapping of the yeast genetic interaction network. Science *303*, 808-813.

Tsukiyama, T., Palmer, J., Landel, C.C., Shiloach, J., and Wu, C. (1999). Characterization of the imitation switch subfamily of ATP-dependent chromatin-remodeling factors in Saccharomyces cerevisiae. Genes & development *13*, 686-697.

van Attikum, H., Fritsch, O., and Gasser, S.M. (2007). Distinct roles for SWR1 and INO80 chromatin remodeling complexes at chromosomal double-strand breaks. The EMBO journal *26*, 4113-4125.

Vary, J.C., Jr., Gangaraju, V.K., Qin, J., Landel, C.C., Kooperberg, C., Bartholomew, B., and Tsukiyama, T. (2003). Yeast Isw1p forms two separable complexes in vivo. Molecular and cellular biology *23*, 80-91.

Xu, H., Boone, C., and Brown, G.W. (2007). Genetic dissection of parallel sister-chromatid cohesion pathways. Genetics *176*, 1417-1429.

Xu, H., Boone, C., and Klein, H.L. (2004). Mrc1 is required for sister chromatid cohesion to aid in recombination repair of spontaneous damage. Molecular and cellular biology *24*, 7082-7090.

Yuan, F., Xu, Z., Yang, M., Wei, Q., Zhang, Y., Yu, J., Zhi, Y., Liu, Y., Chen, Z., and Yang, J. (2013). Overexpressed DNA polymerase iota regulated by JNK/c-Jun contributes to hypermutagenesis in bladder cancer. PloS one *8*, e69317.

Zhao, X., Muller, E.G., and Rothstein, R. (1998). A suppressor of two essential checkpoint genes identifies a novel protein that negatively affects dNTP pools. Molecular cell *2*, 329-340.

Zhou, B.B., and Elledge, S.J. (2000). The DNA damage response: putting checkpoints in perspective. Nature *408*, 433-439.